

**\*\*TITLE\*\****ASP Conference Series, Vol. \*\*VOLUME\*\*, \*\*PUBLICATION YEAR\*\****\*\*EDITORS\*\***

## Three-Dimensional Studies of the Warm Ionized Medium in the Milky Way using WHAM

R. J. Reynolds, L. M. Haffner, and G. J. Madsen

*University of Wisconsin-Madison, Astronomy Department, 475 N. Charter St., Madison, WI 53706*

**Abstract.** The Wisconsin H-Alpha Mapper (WHAM) is a high throughput Fabry-Perot facility developed specifically to detect and explore the warm, ionized component of the interstellar medium at high spectral resolution. It began operating at Kitt Peak, Arizona in 1997 and has recently completed the WHAM Northern Sky Survey (WHAM-NSS), providing the first global view of the distribution and kinematics of the warm, diffuse H II in the Milky Way. This H $\alpha$  survey reveals a complex spatial and kinematic structure in the warm ionized medium and provides a foundation for studies of the temperature and ionization state of the gas, the spectrum and strength of the ionizing radiation, and its relationship to other components of the interstellar medium and sources of ionization and heating within the Galactic disk and halo.

### 1. Introduction

Warm ionized gas is a principal component of the interstellar medium in our Galaxy and others. Its large scale height, mass surface density, and power requirement have significantly modified our understanding of the composition and structure of the interstellar medium and the distribution and flux of ionizing radiation within the disk and halo (e.g., Kulkarni & Heiles 1987; McKee 1990, Reynolds 1991, Ferrière 2001). Although originally detected in the 1960s with radio techniques, subsequent developments in high-throughput Fabry-Perot spectroscopy have shown that the primary source of information about the distribution, kinematics, and other physical properties of this gas is obtained through the detection and study of faint, diffuse interstellar emission lines at optical wavelengths. Presented below are some recent results from the Wisconsin H $\alpha$  Mapper (WHAM), including velocity-interval maps from the recently completed WHAM Northern Sky Survey (WHAM-NSS) of interstellar H $\alpha$  as well as observations of much fainter “diagnostic” emission lines that probe the ionization and excitation state of the gas.

#### 1.1. The Warm Ionized Medium in the Milky Way

Diffuse ionized gas is a major, yet poorly understood component of the interstellar medium, which consists of regions of warm ( $10^4$  K), low-density ( $10^{-1}$  cm $^{-3}$ ), nearly fully ionized hydrogen that occupy approximately 20% of the volume within a 2 kpc thick layer about the Galactic midplane (e.g., Haffner,

Reynolds, & Tufte 1999). Near the midplane, the space averaged density of H II is less than 5% that of the H I. However, because of its greater scale height, the total column density of interstellar H II along high Galactic latitude sight lines is relatively large, 1/4 to 1/2 that of the H I, and one kiloparsec above the midplane, warm H II may be the dominant state of the interstellar medium (Ferrière 2001; Reynolds 1991b). The presence of this ionized medium can have a significant effect upon the interstellar pressure near the Galactic midplane (Cox 1989) and upon the dynamics of hot ( $10^5 - 10^6$  K), “coronal” gas far above the midplane (e.g., Heiles 1990). Miller & Cox (1993) have suggested that this gas is part of a wide spread, warm intercloud medium, while in the McKee & Ostriker (1977) picture of the interstellar medium, this warm H II is located in the outer envelopes of H I clouds, forming the boundary between the clouds and a wide spread, hot (“coronal”) phase.

It is generally believed that the O stars, confined primarily to widely separated stellar associations near the Galactic midplane, are somehow able to account for this widespread gas, not only in the disk but also within the halo, 1-2 kpc above the midplane. However, the nature of such a disk-halo connection is not clear. For example, the need to have a large fraction of the Lyman continuum photons from O stars travel hundreds of parsecs through the disk seems to conflict with the traditional picture of H I permeating much of the interstellar volume near the Galactic plane. It has been suggested that “superbubbles” of hot gas, especially superbubbles that blow out of the disk (“galactic chimneys”), may sweep large regions of the disk clear of H I, allowing ionizing photons from the O stars within them to travel unimpeded across these cavities and into the halo (e.g., Norman 1991). Another possibility is that the Lyman continuum radiation itself is able to carve out extensive regions of H II through low density portions of the H I (e.g., Miller and Cox 1993), perhaps creating photoionized pathways or “warm H II chimneys” that extend far above the midplane (Dove and Shull 1994; Dove, Shull, and Ferrara 2000). Although the existence of superbubbles has long been established (e.g., Heiles 1984), direct observational evidence that such cavities are actually responsible for the transport of hot gas and ionizing radiation up into the Galactic halo is very limited.

Interestingly, even though the source of ionization is believed to be O stars, the temperature and ionization conditions within the diffuse ionized gas appear to differ significantly from conditions within classical O star H II regions. For example, anomalously strong [S II]  $\lambda 6716/\text{H}\alpha$  and [N II]  $\lambda 6584/\text{H}\alpha$ , and weak [O III]  $\lambda 5007/\text{H}\alpha$  emission line ratios (compared to the bright, classical H II regions) indicate a low state of excitation with few ions present that require ionization energies greater than 23 eV (Haffner et al 1999; Rand 1997). This is consistent with the low ionization fraction of helium, at least for the helium near the midplane (Reynolds & Tufte 1995; Tufte 1997; Heiles et al 1996), which implies that the spectrum of the diffuse interstellar radiation field that ionizes the hydrogen is significantly softer than that from the average Galactic O star population. Rand (1997) has also reported lower helium ionization in the H II halo of the edge-on galaxy NGC 891.

Furthermore, it has recently become apparent that O star photoionization models fail to explain observed spatial variations in some of the line intensity ratios. For example, the models do not explain the very large increases in

[N II]/H $\alpha$  and [S II]/H $\alpha$  (accompanied by an increase in [O III]) with distance from the midplane or the observed constancy of [S II]/[N II] (see discussions by Reynolds et al 1999, Haffner et al 1999, and Collins & Rand 2001). The data seem to require the existence of a significant *non-ionizing* source of heat that overwhelms photoionization heating at low densities within the ionized medium (Reynolds et al 1999; Collins & Rand 2001; Otte et al 2001; Bland-Hawthorn, Freeman, & Quinn 1997). Proposed sources include the dissipation of MHD turbulence, Coulomb interactions with cosmic rays, magnetic reconnection, and photoelectric heating by a population of very small grains (see Minter & Spangler 1996; Reynolds et al 1999; Weingartner & Draine 2001).

## 1.2. WHAM

The Wisconsin H-Alpha Mapper (WHAM) is a remotely controlled observing facility, funded by the National Science Foundation and dedicated to the detection and study of faint optical emission lines from the diffuse ionized gas in the disk and halo of the Milky Way (Tufte 1997; Reynolds et al 1998b, Haffner 1998). The WHAM facility consists of a 15 cm aperture dual-etalon Fabry-Perot spectrometer (the largest used in astronomy) coupled to a 0.6 m aperture siderostat, which provide a one-degree diameter beam on the sky and produce a 12 km s<sup>-1</sup> resolution spectrum across a 200 km s<sup>-1</sup> spectral window. The spectral window can be centered on any wavelength between 4800 Å and 7300 Å using a gas (SF<sub>6</sub>) pressure (optical index) control system and a filter wheel. The tandem etalons greatly extend the effective “free spectral range” of the spectrometer, improve the shape of the response profile, and suppress the multi-order Fabry-Perot ghosts, especially those arising from the relatively bright atmospheric OH emission lines within the pass band of the interference filter. A high quantum efficiency (78% at H $\alpha$ ), low noise (3 e<sup>-</sup> rms) CCD camera serves as a multichannel detector, recording the spectrum as a Fabry-Perot “ring image” without scanning (e.g., Reynolds et al 1998b).

The construction and testing of this facility at the University of Wisconsin was completed in September 1996, and WHAM began operating on Kitt Peak in January 1997 (see Fig. 2). Since then, WHAM has been successfully collecting data nearly every clear, dark-of-the-moon period. It has completed as its first major mission a 37,565 spectra H $\alpha$  survey of the northern sky, which has provided the first map of the large scale distribution and kinematics of diffuse interstellar H II that is comparable to earlier 21 cm surveys of H I (§2, below). WHAM is now beginning its second major mission, a comprehensive study of fainter, diagnostic emission lines that trace the excitation and ionization conditions within the gas as well as the strength and spectrum of the ionizing radiation (§3 & §4, below).

## 2. The WHAM Northern Sky H $\alpha$ Survey

From 1997 January through 1998 September, WHAM obtained 37,565 spectra with its 1 degree diameter beam covering the sky on a 0°98/cos $\delta$  × 0°85 grid ( $\ell, b$ ) north of declination  $-30^\circ$ . Figure 1 shows the beam covering pattern for a small portion of the sky survey. The observations were obtained in “blocks”, with each block usually consisting of 49 pointings made sequentially in a boustrophedonic

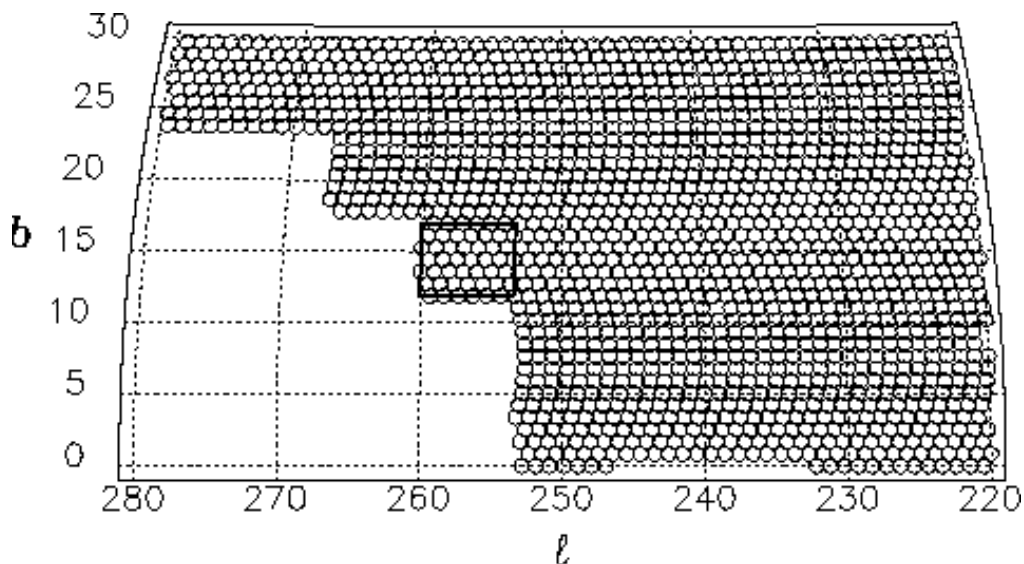


Figure 1. A portion of the sky near the southern declination limit of the survey showing the pattern of WHAM's  $1^\circ$  diameter beams. Observations were obtained as a sequence of “blocks” (outlined), consisting typically of a grid of 49 pointings within in a  $7^\circ \times 6^\circ$  region. The integration time per pointing was 30 s.

raster of seven beams in longitude and seven beams in latitude. Each block took approximately 30 minutes, and from one to twenty blocks were observed in a night. The absence or presence of block boundary features in the completed survey map provide an excellent gauge of the systematic errors associated with observations taken on different nights and different times of the year. The radial velocity interval for the survey was limited to  $\pm 100 \text{ km s}^{-1}$  with respect to the LSR. This range includes nearly all of the interstellar emission at high latitudes except the  $\text{H}\alpha$  associated with High Velocity H I Clouds (HVCs), which by definition have radial velocities  $|v| > 80 \text{ km s}^{-1}$ .

Figure 2 shows the resulting survey maps, including views of the total  $\text{H}\alpha$  intensity in addition to velocity interval maps. Interstellar  $\text{H}\alpha$  emission extends over virtually the entire sky, with blobs and filaments of enhanced  $\text{H}\alpha$  superposed on a more diffuse background. The highest  $\text{H}\alpha$  intensities are found near the Galactic equator, with a general decrease toward the poles. Some of the new features revealed by this survey are discussed by Haffner (2001), Reynolds et al (2001a), and Haffner, Reynolds, & Tufte (1998).

### 3. Mapping the Excitation and Ionization State of the Gas

With the  $\text{H}\alpha$  survey providing a picture of the overall distribution and kinematics of the warm ionized medium, the detection and study of other emission lines can be used to probe the physical conditions within the gas. One of the outstanding questions is the source of the ionization and heating. Valuable clues

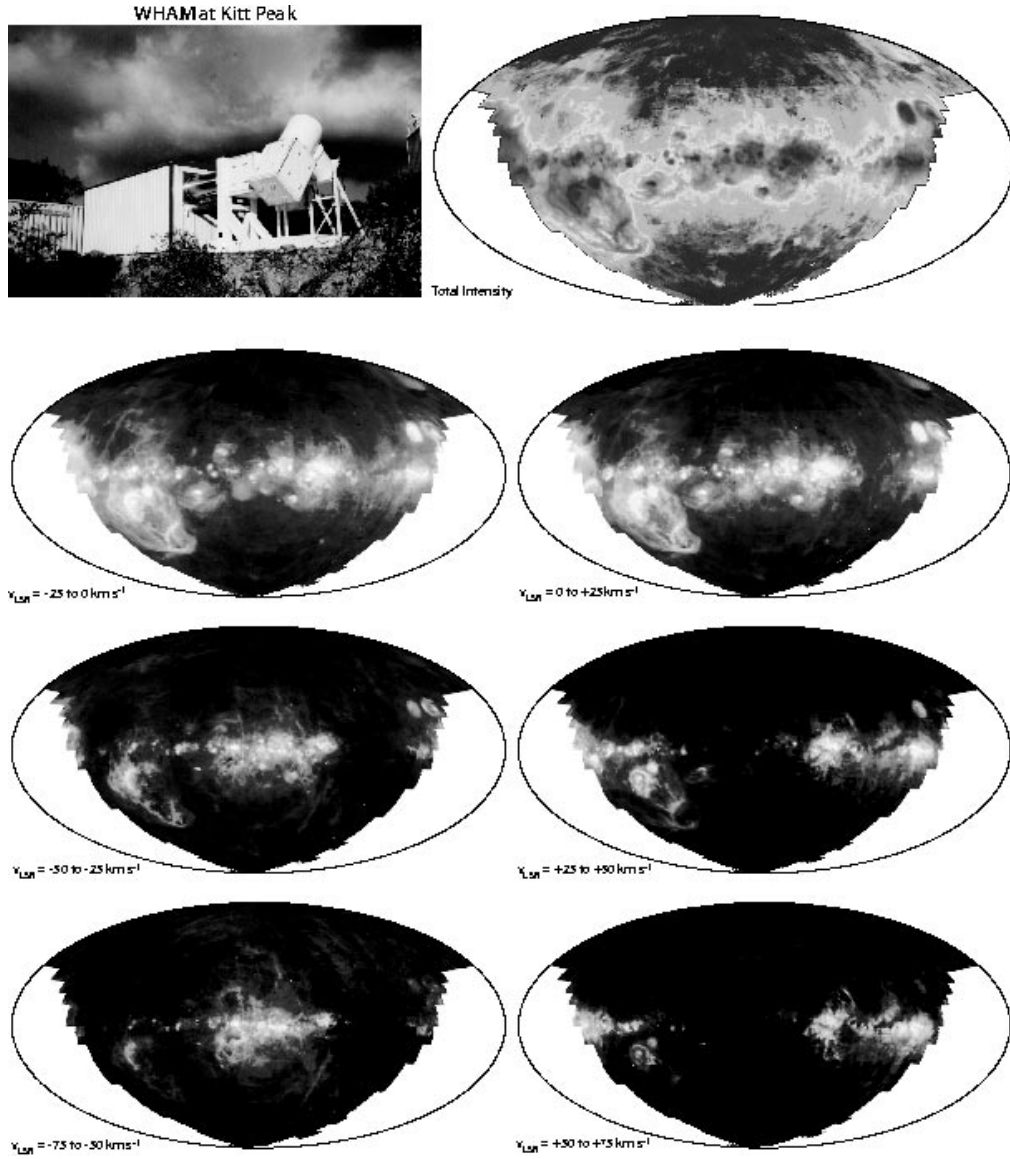


Figure 2. The WHAM facility at Kitt Peak plus H $\alpha$  total intensity and velocity interval maps from its recently completed Northern Sky Survey, revealing for the first time the distribution and kinematics of the diffuse H II over the sky. All maps are centered at  $\ell = 120^\circ$ . These data have been released to the community and are available at <http://www.astro.wisc.edu/wham/>.

are contained in the emission line spectrum, which is characterized by high  $[\text{N II}] \lambda 6584/\text{H}\alpha$  and  $[\text{N II}] \lambda 6716/\text{H}\alpha$  and low  $[\text{O III}] \lambda 5007/\text{H}\alpha$  and  $\text{He I } \lambda 5876/\text{H}\alpha$  line intensity ratios relative to the ratios observed in bright H II regions around O stars (e.g., Rand 1997, 1998; Haffner et al 1999). This implies ionization and excitation conditions in the diffuse ionized gas that differ significantly from conditions in the classical H II regions. Not only are the conditions different, but they vary significantly with distance from the midplane, from sightline to sightline, and even from one velocity component to the next along a single sightline (e.g., Haffner et al 1999; Collins and Rand 2001; see also Figs. 3 and 4 below).

To map these variations throughout the nearby spiral arms and to explore how the observed differences in conditions are related to the structures revealed by the WHAM-NSS and to the known sources of ionization, WHAM has begun to map portions of the Galaxy in the  $[\text{N II}]$  and  $[\text{S II}]$  lines. The power of these observations is illustrated in Figure 3 below, from Haffner et al (1999), who used WHAM to map  $[\text{N II}]$  and  $[\text{S II}]$  over a limited ( $30^\circ \times 40^\circ$ ) region of the sky that sampled parts of the Local (Orion) and Perseus arms. These observations by WHAM confirmed for the Milky Way, and have extended to much fainter emission, similar trends noticed in emission line observations of other galaxies—namely, a dramatic increase in  $[\text{N II}]/\text{H}\alpha$  and  $[\text{S II}]/\text{H}\alpha$  with increasing distance  $|z|$  above the midplane, with relatively small (but statistically significant) variations in  $[\text{S II}]/[\text{N II}]$ , which are inconsistent with pure photoionization models (see Collins & Rand 2001; Otte et al 2001).

Haffner et al (1999) and Reynolds et al (1999) have pointed out that these observations can be readily explained if the variations in the forbidden line ratios are due primarily to variations in the electron temperature ( $\Delta T_e \approx 2000$  K to 3000 K) of the gas rather than to variations in the ionization parameter. This would naturally explain the near constancy of  $[\text{S II}]/[\text{N II}]$ , for example, since these optical transitions of  $\text{S}^+$  and  $\text{N}^+$  have nearly identical excitation energies. If true, variations in  $[\text{N II}]/\text{H}\alpha$  are tracing variations in the temperature of the gas, and the small variations in  $[\text{S II}]/[\text{N II}]$  are reflecting variations in the ionization state (i.e.,  $\text{S}^+/\text{S}$ ; see discussion by Haffner et al 1999). Recent follow up observations of the Milky Way (WHAM observations using the temperature diagnostic  $[\text{N II}] \lambda 5755/[\text{N II}] \lambda 6584$ ; Reynolds et al 2001b) and other galaxies (Collins & Rand 2001; Otte et al 2001) have provided support for this idea, although it may not apply in all cases (Martin & Kern 2001).

#### 4. Detecting Much Fainter Emission Lines

WHAM also provides the opportunity to detect and study emission lines from the diffuse interstellar medium that are too faint to have been detected previously, such as  $[\text{O I}] \lambda 6300$ ,  $\text{He I } \lambda 5876$ ,  $[\text{N II}] \lambda 5755$ , and  $[\text{O III}] \lambda 5007$ . The intensities, widths, and radial velocities of these lines contain unique additional information about the ionizing radiation and conditions within the emitting gas, and they can place strong constraints on theoretical models. For example, these lines probe:

**hydrogen ionization fraction:** The intensity of the  $[\text{O I}] \lambda 6300$  line relative to  $\text{H}\alpha$ , when combined with the electron temperature (e.g.,  $[\text{N II}] \lambda$

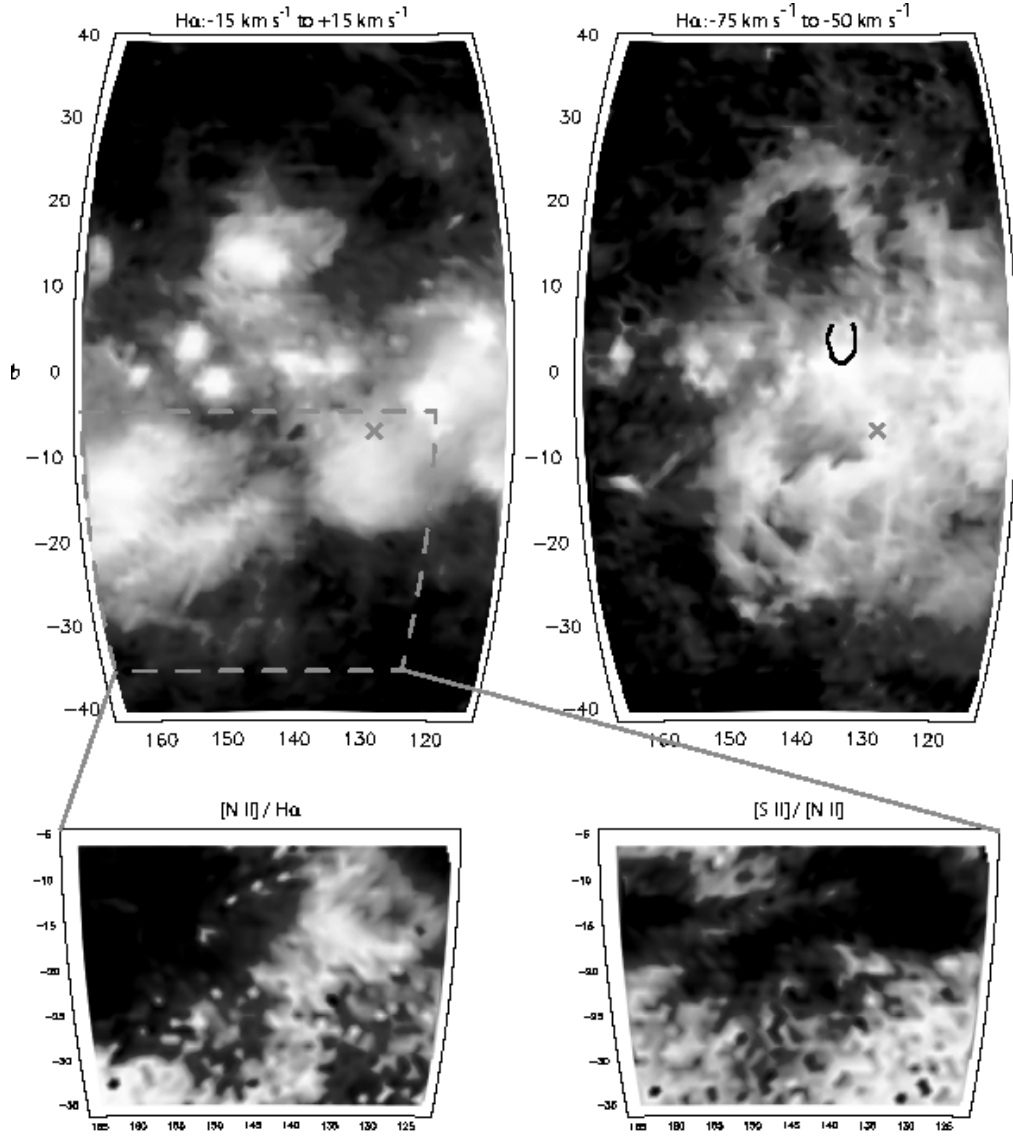
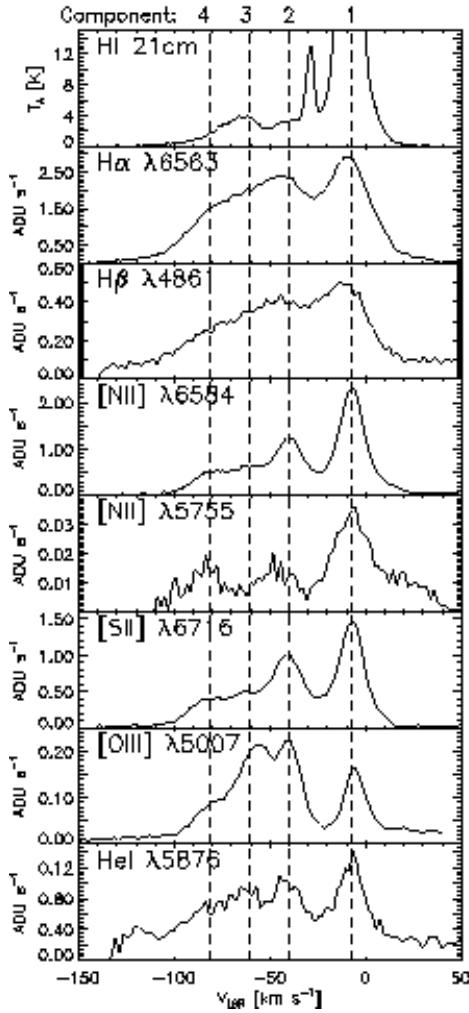


Figure 3. At the top of the figure are two WHAM velocity interval maps of a one-steradian portion of the sky showing emission from the Local Orion arm at  $V_{lsr} = -15$  to  $+15$  km s<sup>-1</sup> and from the more distant Perseus arm at  $V_{lsr} = -75$  to  $-50$  km s<sup>-1</sup>. The large loop in the upper half of this second map is part of a superbubble that appears to have blown out into the Galactic halo above the “W4 chimney” (the horseshoe schematic) associated with the Cas OB6 association (Normandeau et al 1996; Reynolds et al 2001a). The “x” denotes the sightline for the observations presented in Fig. 4. Also shown for the region within the dashed boundary are  $-15$  to  $+15$  km s<sup>-1</sup> maps of  $[N II]/H\alpha$  and  $[S II]/[N II]$ , which are believed to trace variations in the excitation ( $T_e$ ) and ionization ( $S^+/S$ ) of the  $H\alpha$  emitting gas, respectively.



Characteristic Relative Line Intensities

Line	WTM	O Star HII Regions
H $\alpha$	1.00	1.00
H $\beta$	0.25	0.25
[NII] $\lambda$ 6583	0.4	0.2
[NII] $\lambda$ 5755	0.004	0.001
[SII] $\lambda$ 6716	0.3	0.06
[OIII] $\lambda$ 5007	0.06	0.3
HeI $\lambda$ 5876	0.03	0.05

Figure 4. The H I 21 cm spectrum from Leiden/Dwingeloo plus spectra of seven optical emission lines from WHAM toward  $\ell = 130.0$ ,  $b = -7.5$  (denoted by an “ $\times$ ” in Fig. 3). Except for the narrow H I component at  $-20 \text{ km s}^{-1}$ , each of the optically emitting clouds along this sightline appears to have a corresponding emission feature in the 21 cm spectrum. Note the variations in physical conditions along the sightline, for example, the relatively high [O III] in component 3 relative to component 1 when compared to [S II] or [N II].



5755/[N II]  $\lambda 6584$ ; see below), measures the hydrogen ionization fraction (i.e., the ionization parameter) within the emitting gas. This diagnostic tightly constrains the possible mechanisms of ionization and provides important information about the relationship between the H II and the H I within the diffuse interstellar medium (Domgörgen & Mathis 1994). The first detections of diffuse, interstellar [O I] (toward three sightlines with WHAM) appear to rule out the existence of warm, partially ionized H I clouds, for example, and have revealed significant variations in [O I]/H $\alpha$  from cloud to cloud (Reynolds et al 1998a).

**spectrum of the ionizing radiation:** The He I  $\lambda 5876$ /H $\alpha$  recombination line ratio probes the hardness of the ionizing spectrum. The relatively weak He I/H $\alpha$  intensity ratios in the warm ionized medium compared to O star H II regions (Tufté 1997; Heiles et al 1996; Rand 1997) imply either a reprocessing of the radiation from O stars or a significant “new” source of soft Lyman continuum photons that has not been recognized (B stars? See Cassinelli et al 1995).

**electron temperature:** The ratio [N II]  $\lambda 5755$ /[N II]  $\lambda 6584$  is an unambiguous electron temperature diagnostic for ionized regions (Osterbrock 1989). The  $\lambda 5755$  emission has been detected by WHAM in multiple velocity components toward a diffuse background sightline (see Fig. 4), revealing that the electron temperature in the diffuse H II is approximately 2000 K warmer than that in bright, classical O star H II regions (Reynolds et al 2001b). This result lends strong support for the existence of an additional heating source within the low density gas (§1.1 above).

**state of higher ions:** Observed variations in the weak [O III]  $\lambda 5007$  line relative to lines from ions of lower ionization state are a sensitive probe of changes in the state of the rarer, higher ions in the gas (e.g., Rand 1997). For example, toward  $130^\circ, -7.5^\circ$  (Fig. 4), [O III]/[S II] varies considerably from one velocity component to the next. Comparisons with the [N II]  $\lambda 5755$  and [N II]  $\lambda 6584$  profiles indicate that the relatively strong [O III] in velocity component 3 and weak [O III] in component 1 cannot be due to temperature differences, but rather must reflect significant variations in the abundance of the  $O^{++}$  ion among the different clouds.

#### 4.1. The Relationship between H I and H II in the ISM, IVCs, and HVCs

Along sightlines away from the Galactic midplane, there appears to be a generally close relationship, both kinematically and spatially, between the diffuse H II and “warm” (broad component) H I clouds, including the distinct complexes of gas at intermediate and high velocities (e.g., Reynolds et al 1995; Haffner et al 2001). In Figure 4, for example, except for the narrow H I component at  $-20 \text{ km s}^{-1}$ , each of the optically emitting clouds along the  $\ell = 130.0, b = -7.5$  sightline appears to have a corresponding emission feature in the 21 cm spectrum. This close relationship between the diffuse H II and the warm H I phase is apparent in many other sightlines (e.g., Haffner et al 2001; Hausen et al 2002; Reynolds et al 1995). Therefore, these emission line observations impact not only our understanding of the ionized gas, but also provide a new insight into the nature of

H I clouds. The intensity of the  $H\alpha$  emission provide a measure of the ionizing flux incident on the cloud (Tufté et al 1998), while the other fainter lines probe the spectrum of the radiation and the properties of the cloud's associated H II.

Although their existence has been known for many years, the origin of High Velocity Clouds (HVCs) is still not clear (e.g., Wakker 2001). This is due at least in part to the fact that, until relatively recently, HVCs could be studied in emission only via the 21 cm line. The detection of HVCs in optical emission lines has provided a fresh new approach to these enigmatic objects (e.g., Tufté et al 1998; S. Tufté, in preparation), resulting in information about their distances, abundances, origin, and the environment in which they are located (Wakker et al 1999; Bland-Hawthorn & Maloney 1999; Weiner & Williams 1996).

## 5. Exploring the Influence of Extinction on Interstellar Emission Lines

Interstellar extinction is significant within about  $5^\circ$ – $10^\circ$  of the Galactic equator, where the optical depth through the disk at  $H\alpha$  reaches unity or greater. To measure the influence of extinction on the low latitude portion of the WHAM-NSS, we have begun mapping the Galactic plane in  $H\beta$ . Because the emission is kinematically resolved, these observations make it possible to map the effect of extinction (i.e., the  $H\beta/H\alpha$  ratio) as a function of position along the line of sight and to explore with numerical radiation transfer models the absorption and scattering of the diffuse interstellar emission within the Galactic disk (K. Wood, private communication; Wood & Reynolds 1999). Many low latitude WHAM-NSS spectra between longitudes  $15^\circ$  and  $35^\circ$  show emission out to radial velocities of  $+80 \text{ km s}^{-1}$  or greater, indicating that WHAM can probe into the inner Galaxy to a distance of 4 kpc or more.

## 6. High Angular Resolution ( $3'$ ) Imaging

A relatively recent optical-mechanical upgrade has given WHAM an imaging capability, making it possible to obtain deep, high angular resolution ( $3'$ ), very narrow band images having a selectable band width from 20 to  $200 \text{ km s}^{-1}$  ( $0.4$  to  $4 \text{ \AA}$ ) within its  $1^\circ$  diameter beam. At  $H\alpha$ , a signal-to-noise ratio of 9 is reached for 0.5 R per  $3'$  pixel in a 25 minute exposure. Longer integrations times are required for [N II] and [S II] images. By revealing any structure within WHAM's  $1^\circ$  diameter beam, such imaging observations can be used to interpret properly interstellar emission line and absorption line studies toward the same sightline. In addition, these high spatial resolution observations can probe the small scale structure of filaments and “WHAM point sources” (large, low surface brightness planetary nebulae?) discovered in the survey, as well as regions that overlap with high angular resolution 21 cm maps (e.g., Arecibo and the DRAO CGPS). “WHAM deep fields” in high latitude directions may provide insight into the small scale structure (if any) in the properties and kinematics of the diffuse ionized regions.

## 7. Summary

The development of high throughput, high spectral resolution Fabry-Perot spectroscopy has established that faint, diffuse interstellar emission lines at optical wavelengths contain a wealth of new information about the interstellar medium that cannot be obtained through other techniques at other wavelengths. The WHAM H $\alpha$  survey plus the detection of fainter nebular lines reveal a complexity not only in the structure and kinematics of the warm ionized medium, but also in its excitation and ionization conditions. Studies of this weak emission have begun to shed new light on the nature of the interstellar medium and the principal sources of ionization and heating within the disk and halo of the Galaxy.

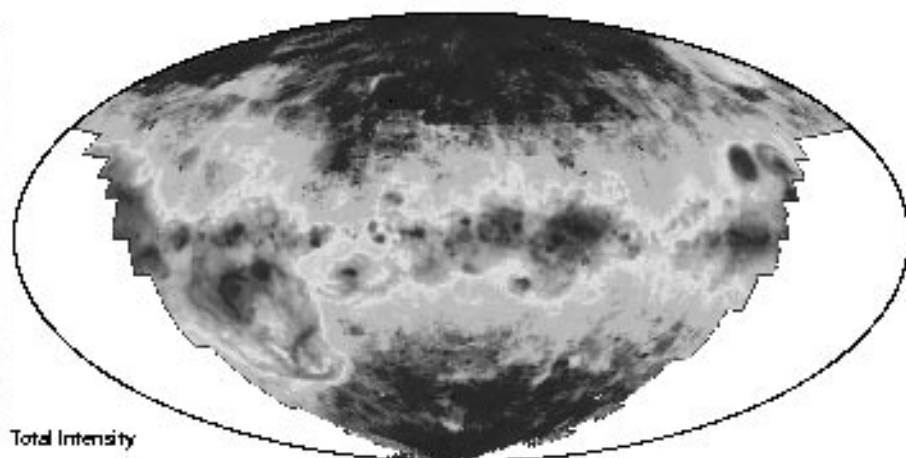
**Acknowledgments.** This work was supported by the National Science Foundation grant AST96 19424. We are also grateful to S. L. Tufte, K. Jaehnig, N. R. Hausen, J. Percival, R. Pifer, B. Babler, M. Quigley, and T. Tillemann for their contributions to WHAM, the survey observations, and the survey data reduction.

## References

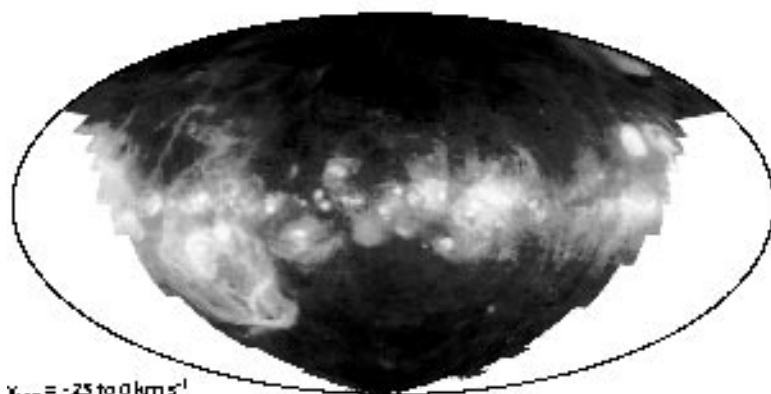
- Bland-Hawthorn, J., Freeman, K. C., & Quinn, P. J. 1997, ApJ 490, 143  
 Bland-Hawthorn, J. & Maloney, P. R. 1999, ApJ 522, 81  
 Cassinelli, J. P., Cohen, D. H., Macfarlane, J. J., Drew, J. E., Lynas-Gray, A. E., Hoare, M. G., Vallergha, J. V., Welsh, B. Y., Vedder, P. W., Hubeny, I., & Lanz, T. 1995, ApJ 438, 932.  
 Cox, D. P. 1989, in *Structure and Dynamics of the Interstellar Medium*, eds. G. Tenorio-Tagle, M. Moles, & J. & J. Melnick (Springer-Verlag), p. 500  
 Collins, J. A. and Rand, R. J. 2001, ApJ 551, 57  
 Domgörgen, H. & Mathis, J. S. 1994, ApJ 428, 647  
 Dove, J. B. & Shull, J. M. 1994, ApJ 430, 222  
 Dove, J. B., Shull, J. M., and Ferrara, A. 2000, ApJ 531, 856  
 Ferrière, K. M. 2001, Reviews of Modern Physics, October 2001  
 Haffner, L. M. 1998, PhD Thesis, University of Wisconsin-Madison  
 Haffner, L. M. 2001, in *Tetons 4: Galactic Structure, Stars, & the Interstellar Medium*, ASP Conference Series Vol. 231, eds., C. E. Woodward, M. D. Biscay, and J. M. Shull, p. 345  
 Haffner, L. M., Reynolds, R.J., and Tufte, S.L. 1998, ApJ 501, L83  
 Haffner, L. M., Reynolds, R.J., and Tufte, S.L. 1999, ApJ 523, 223  
 Haffner, L. M., Reynolds, R.J., and Tufte, S.L. 2001, ApJ 556, L33  
 Hausen, N. R., Reynolds, R. J., Haffner, L. M., & Tufte, S. L. 2002, ApJ, in press  
 Heiles, C. 1984, ApJS 55, 585  
 Heiles, C. 1990, ApJ 354, 483  
 Heiles, C., Koo, B.-C., Levenson, N. A., & Reach, W. T. 1996, ApJ 462, 326

- Kulkarni, S. R. & Heiles, C. 1987, in *Interstellar Processes*, eds. D. J. Hollenbach & H. A. Thronson, Jr. (Dordrecht:Ridel), p. 87
- Martin, C. & Kern, B. 2001, ApJ 555, 258
- McKee, C. F. 1990, in *The Evolution of the Interstellar Medium*, ed. L. Blitz (ASP Conference Series Vol. 12), p. 3
- McKee, C. F. & Ostriker, J. P. 1977, ApJ 218, 148
- Miller, W. W., III & Cox, D. P. 1993, ApJ 417, 579
- Minter, A. H. & Spangler, S. R. 1996, ApJ 458, 194
- Norman, C. 1991, in *The Interstellar Disk-Halo Connection in Galaxies*, IAU Symp. No. 144, ed. H. Bloemen (Dordrecht:Kluwer), p. 337
- Normandeau, M., Tatlor, A. R., & Dewdney, P. E. 1996, Nature 380, 687
- Osterbrock, D. E. 1989, *Astrophysics of Gaseous Nebula and Active Galactic Nuclei*, (Mill Valley:University Science Books)
- Otte, B., Reynolds, R. J., Gallagher, J. S., III, and Ferguson, A. M. N. 2001, ApJ, in press
- Rand, R. J. 1997, ApJ 474, 129
- Rand, R. J. 1998, ApJ 501, 137
- Reynolds, R. J. 1991, in *The Interstellar Disk-Halo Connection in Galaxies*, IAU Symp. No. 144, ed. H. Bloemen (Dordrecht:Kluwer), p.67
- Reynolds, R. J., Haffner, L.M., and Tufte, S.L. 1999, ApJ 525, L21
- Reynolds, R. J., Hausen, N.R., Tufte, S.L., and Haffner, L.M. 1998a, ApJ 494, L99
- Reynolds, R. J., Sterling, N., Haffner, L. M. 2001a, ApJ 558, L101
- Reynolds, R. J., Sterling, N., Haffner, L.M., and Tufte, S.L. 2001b, ApJ 548, L221
- Reynolds, R. J. & Tufte, S. L. 1995, ApJ 439, L17
- Reynolds, R. J., Tufte, S.L., Haffner, L.M., Jaehnig, K., Percival, J. 1998b, PASA, 15, 14
- Reynolds, R. J., Tufte, S. L., Kung, D. T., McCullough, P. R., & Heiles, C. 1995, ApJ 448, 715
- Tufte, S. L. 1997, PhD Thesis, University of Wisconsin-Madison
- Tufte, S. L., Reynolds, R. J., and Haffner, L. M. 1998, ApJ 504, 773
- Wakker, B.P. 2001, ApJS 136, 463
- Wakker, B. P., Howk, J. C., Savage, B. D., van Woerden, H., Tufte, S. L., Schwarz, U. J., Benjamin, R., Reynolds, R. J., Peletier, R. F., Kalberla, P. M. W. 1999, Nature 402, 388
- Weiner, B. J. & Williams, T. B. 1996, AJ 111, 1156
- Weingartner, J. C., & Draine, B. T. 2001, ApJS 143, 263
- Wood, K. and Reynolds, R.J. 1999, ApJ 525, 799

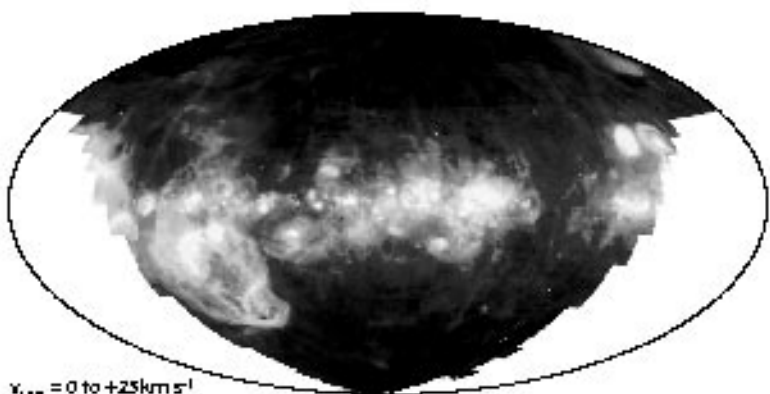
WHAM at Kitt Peak



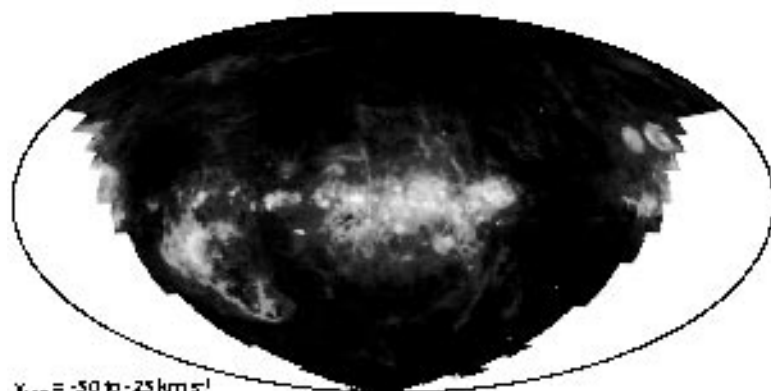
Total Intensity



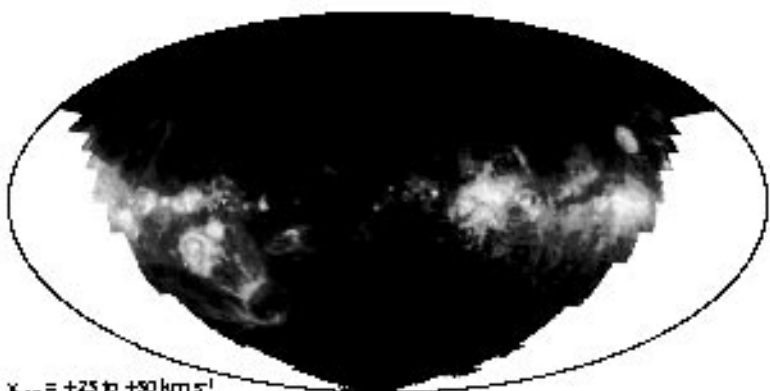
$v_{\text{LSR}} = -25 \text{ to } 0 \text{ km s}^{-1}$



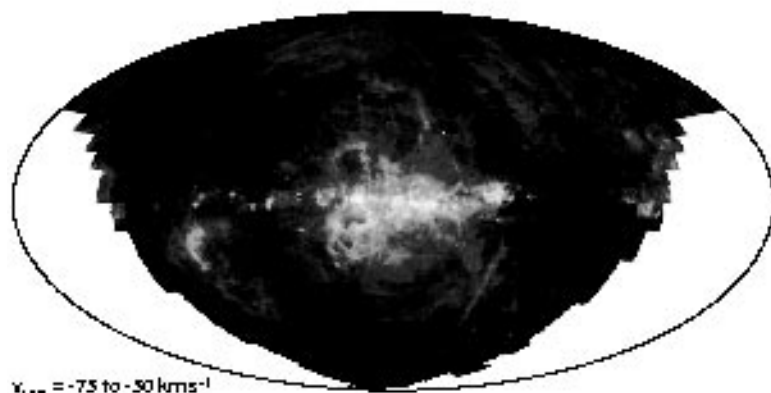
$v_{\text{LSR}} = 0 \text{ to } +25 \text{ km s}^{-1}$



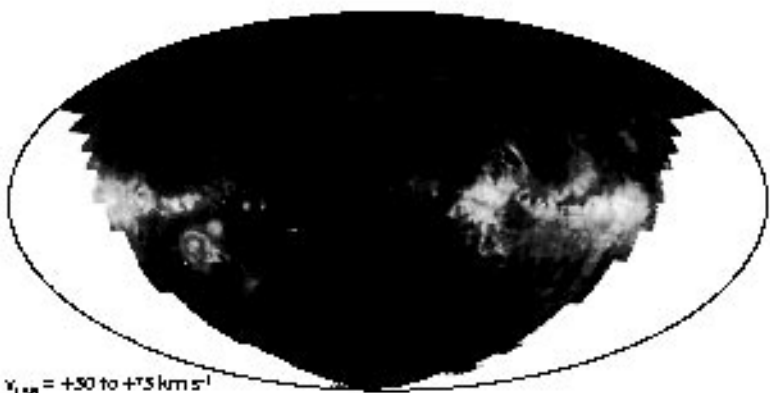
$v_{\text{LSR}} = -50 \text{ to } -25 \text{ km s}^{-1}$



$v_{\text{LSR}} = +25 \text{ to } +50 \text{ km s}^{-1}$



$v_{\text{LSR}} = -75 \text{ to } -50 \text{ km s}^{-1}$



$v_{\text{LSR}} = +50 \text{ to } +75 \text{ km s}^{-1}$

